

1 **A chironomid-based record of temperature variability during the**
2 **past 4000 years in northern China and its possible societal**
3 **implications**

4 Haipeng Wang ^{1,2}, Jianhui Chen ^{2*}, Shengda Zhang ³, David D. Zhang ^{4,3}, Zongli Wang ², Qinghai
5 Xu ⁵, Shengqian Chen ², Shijin Wang ¹, Shichang Kang ¹, and Fahu Chen ²

6

7 *¹State Key Laboratory of Cryospheric Science, Northwest Institute of Eco-Environment and*
8 *Resources, Chinese Academy of Sciences, Lanzhou 730000, China*

9 *²MOE Key Laboratory of Western China's Environmental Systems, College of Earth*
10 *Environmental Sciences, Lanzhou University, Lanzhou 730000, China*

11 *³Department of Geography, The University of Hong Kong, Hong Kong, China*

12 *⁴School of Geographical Sciences, Guangzhou University, Guangzhou 510000, China*

13 *⁵Institute of Nihewan Archaeology Research, Hebei Normal University, Shijiazhuang 050024,*
14 *China*

15 ** Author for correspondence (email: jhchen@lzu.edu.cn)*

16

17 **Abstract:** Long-term, high-resolution temperature records which combine an unambiguous
18 proxy and precise dating are rare in China. In addition, the societal implications of past
19 temperature change on a regional scale have not been sufficiently assessed. Here, based on the

20 modern relationship between chironomids and temperature, we use fossil chironomid
21 assemblages in a precisely-dated sediment core from Gonghai Lake to explore temperature
22 variability during the past 4000 years in northern China. Subsequently, we address the
23 possible regional societal implications of temperature change through a statistical analysis of
24 the occurrence of wars. Our results show that: (1) the mean annual temperature (TANN) was
25 relatively high from 4000-2700 cal yr BP, decreased gradually from 2700-1270 cal yr BP, and
26 then fluctuated during the last 1270 years. (2) A cold climatic event in the Era of Disunity, the
27 Sui-Tang Warm Period (STWP), the Medieval Warm Period (MWP) and the Little Ice Age
28 (LIA) can all be recognized in the paleotemperature record, as well as in many other
29 temperature reconstructions in China. This suggests that our chironomid-inferred temperature
30 record for the Gonghai Lake region is representative. (3) Local wars in Shanxi Province,
31 documented in the historical literature during the past 2700 years, are statistically
32 significantly correlated with changes in temperature, and the relationship is a good example
33 of the potential societal implications of temperature change on a regional scale.

34 **Keywords:** chironomids, temperature change, northern China, late-Holocene, societal
35 implications

36

37 **1 Introduction**

38 Climate change presents new and significant challenges for human society, including the
39 need to understand and respond to the possible dangers (Stocker et al., 2013). Since the past is
40 the key to the present and the future, the study of past temperature changes is becoming
41 increasingly important for improving our ability to predict the long-term trends of regional
42 and global climate change, and to explore the relationship between climate change and human

43 society.

44 East Asia, a densely populated region, has attracted much research attention focused on
45 documenting the frequency and amplitude of past climate changes. While the Holocene
46 variability of the precipitation associated with the East Asian summer monsoon (EASM) has
47 been discussed in detail (e.g., Hu et al., 2008; Cai et al., 2010; F.H. Chen et al., 2015; J.B. Liu
48 et al., 2015; J.H. Chen et al., 2016; J.B. Liu et al., 2017), studies of temperature change on
49 different temporal and spatial scales may provide deeper insights to past climate fluctuations
50 and facilitate the prediction of future climate change. During the past few decades, various
51 studies have reconstructed temperature change on different time-scales in northern China,
52 using for example pollen (e.g., Xu et al., 2010; Wen et al., 2010), glycerol dialkyl glycerol
53 tetraethers (GDGTs) (e.g., Gao et al., 2012; Jia et al., 2013; Peterse et al., 2014), stalagmites
54 (Tan et al., 2003), and historical archives (Ge et al., 2003). However, many of these
55 temperature records have significant limitations: for example, pollen assemblages are
56 regarded as a precipitation indicator in many records in northern China (e.g., F.H. Chen et al.,
57 2015; Zhao et al., 2010), the resolution of GDGTs records is too low (although their
58 environmental significance is relatively unambiguous), and the timescales of the stalagmite
59 records from Shihua Cave, and of historical documents from East China, are too short, even if
60 they are accurately dated. All these factors impede our understanding of paleotemperature
61 variability during the Holocene, and in addition there is a mismatch between model
62 simulations of a cooler-than-baseline annual temperature series during the late Holocene
63 compared to the present climate (Jiang et al., 2012) and multi-proxy reconstructions of the
64 mid-Holocene megathermal in China (e.g., Shi et al., 1993; S. Wang et al., 2001; Peterse et al.,
65 2011; Huang et al., 2013). Thus, a long-term, high-resolution paleotemperature reconstruction,
66 using an unequivocal proxy with a robust chronology, is needed.

67 Chironomids, benthic invertebrates, are recognized as a reliable paleotemperature proxy
68 because of their stenotopic and environmentally-sensitive characteristics (Walker et al., 1991;
69 Levesque et al., 1997; Brooks et al., 2007; Brooks et al., 2012a). Many modern chironomid
70 training sets have been established and used for paleoenvironmental reconstruction
71 (especially paleotemperature) worldwide (e.g., Walker and Cwynar, 2006; Rees et al., 2008;
72 Eggermont et al., 2010; Heiri et al., 2011; Nazarova et al., 2011; Massaferro and
73 Larocque-Tobler, 2013). The paleoenvironmental application of chironomid analysis is
74 relatively recent in China, and studies have concentrated mainly on lake ecology, including
75 analysis of total phosphorus in the middle and lower reaches of the Yangtze River (E.L.
76 Zhang et al., 2006), salinity on the Tibetan Plateau (E.L. Zhang et al., 2007; J.H. Chen et al.,
77 2009), lake water-depth in the arid region of northwest China (J.H. Chen et al., 2014), and
78 precipitation near the EASM boundary (H.P. Wang et al., 2016). Currently, there is only one
79 chironomid-based temperature record, which was obtained from the southeastern Tibetan
80 Plateau (E.L. Zhang et al., 2017a and 2017b).

81 Here, we present the results of a study of chironomid assemblages in a sediment core from
82 Gonghai Lake in northern China, with the aim of reconstructing regional temperature
83 variability during the past 4000 years in northern China. Gonghai Lake, a freshwater
84 closed-basin lake in Shanxi Province (Fig. 1a), was previously shown to be suitable for
85 chironomid studies (H.P. Wang et al., 2016). A modern calibration data set consisting of 44
86 fresh water bodies in the area has been developed by H.P. Wang and co-workers (2016).
87 Although this data set suggested that chironomid assemblages in the region responded
88 significantly to fluctuations in water depth since the last deglaciation (H.P. Wang et al., 2016),
89 the existence of several typical stenothermal species (e.g., *Hydrobaenus conformis*-type,
90 *Dicrotendipes nervosus*-type) in the fossil sequence (H.P. Wang et al., 2016), which are
91 sensitive to temperature variability on various time scales (Cranston et al., 1983; Brodin, 1986;

92 Watson et al., 2010; Brooks and Heiri, 2013), offers great potential for paleotemperature
93 reconstruction in the area. In addition, as well as having significant regional environmental
94 effects, past climate change may also have triggered human societal crises (D.D. Zhang et al.,
95 2015). Numerous studies have demonstrated a strong temporal relationship between societal
96 crises and climate change, and a recent study indicated that climate change (especially
97 temperature) was the ultimate cause of a large-scale human crisis in preindustrial Europe and
98 the Northern Hemisphere (D.D. Zhang et al., 2011). However, most of the previous research
99 has focused on the human societal response to climate change on a large spatial scale (e.g.,
100 Tan et al., 2011a) and the response on a regional scale has rarely been considered. The aim of
101 the present study is to reconstruct temperature changes during the past 4000 years in northern
102 China using stenothermic chironomid taxa, and to test the hypothesis that human societal
103 crises were an indirect consequence of temperature fluctuations at the regional scale.
104 Therefore, we (i) identify typical warm- and cold-preference chironomid taxa as temperature
105 indicators, based on the modern calibration set and previous ecological understanding from
106 the literature; (ii) estimate past temperature variability by analyzing the percentage changes in
107 warm- and cold-preference taxa, and validate its reliability; and (iii) compare the temperature
108 record with the documented occurrence of wars in Shanxi Province.

109 **2 Regional setting**

110 Gonghai Lake (38°54' N, 112°14' E; 1,860 m.a.s.l), an alpine freshwater lake, is situated
111 on the northeastern margin of the Chinese Loess Plateau (Fig. 1a). The lake is oval-shaped
112 and has a surface area of ~0.36 km², a maximum water depth of around 10 m, and a flat
113 bottom-topography (Fig. 1b). The lake may have been formed by tectonic activity at around
114 ~16 ka BP (X. Wang et al., 2014). On average, 77 % of the 445 mm of modern annual
115 precipitation occurs from June to September and is the major water source since the lake is

116 hydrologically closed. Modern mean monthly temperature in the region ranges between
117 -14 °C and +23 °C. In 2009, a 9.42-m-long sediment core (GH09B) was taken in a water
118 depth of 8.96 m (Fig. 1b) using a Uwitec Piston Corer. The core was sliced at 1-cm intervals,
119 freeze-dried and stored at 4 °C in the laboratory. In the present study, 109 samples from the
120 upper 541 cm were processed for chironomid analysis. Several adjacent samples which
121 produced fewer than 30 head capsules were amalgamated. A total of 63 samples was included
122 and used for temperature analysis, of which 44 samples contained more than 40 head capsules
123 and 19 samples contained 30-40 head capsules, representing time intervals varying between
124 50 and 100 years and spanning the past ca. 4000 years.

125

126

Figure 1

128

129

130 **3 Chronology**

131 The age-depth model for Gonghai Lake core GH09B (F.H. Chen et al., 2015) was used in
132 this study. Figure 2 shows the chronology for the last 4000 years. In the age-depth model for
133 core GH09B, 25 accelerator mass spectrometry (AMS) ¹⁴C dates were obtained from
134 terrestrial plant macrofossils, calibrated using the IntCal09 calibration curve (Reimer et al.,
135 2009), and used for Bayesian age-depth modelling (Bronk Ramsey, 2008).

136

137

138

Figure 2

139

140

141 **4 Materials and methods**

142 4.1 Chironomid samples

143 For each sample, chironomid remains were extracted from 1-5 g of freeze-dried sediment.
144 The preparation procedure followed the standard techniques described in Brooks *et al.* (2007).
145 The sediments were deflocculated in warm 10 % KOH for about 15 minutes, and then sieved
146 with 212 μm and 90 μm mesh sieves. Head capsules were hand-picked from the sieve
147 residues under a stereomicroscope at $\times 20$ -40 magnification, and mounted on slides, ventral
148 side up, in Hydromatrix beneath a 6-mm coverslip. Chironomid head capsules were identified
149 to the highest possible taxonomic resolution under a compound microscope at $\times 100$ -400
150 magnification with reference to Wiederholm (1983), Rieradevall and Brooks (2001), Brooks
151 *et al.* (2007), Walker (2007), and the chironomid collections housed at the Natural History
152 Museum, London.

153 4.2 Calibration set

154 The modern calibration set from around Gonghai Lake obtained by H.P. Wang and
155 coworkers (2016) was used to identify temperature-sensitive chironomid taxa in the region.
156 The data set comprises 44 water bodies in northern China (Fig. 3a), samples from only 30 of
157 which contained sufficient chironomid head capsules for analysis.

158 Mean annual temperature (TANN), mean summer temperature (summer Tem), and the
159 mean temperatures for June (June Tem), July (July Tem) and August (August Tem) were
160 interpolated from meteorological data from 2001-2011 ([Dataset of monthly values of climate
161 data from Chinese surface station, 2017](#); Zhao et al., unpublished data). It should be noted that
162 the surface of Gonghai Lake freezes in winter which disrupts the linear relationship between
163 water temperature and air temperature. Moreover, the winter season is not the growing season
164 of chironomids (Armitage et al., 1995), and therefore the mean temperature of the winter
165 months was not included in the numerical analysis.

166 4.3 Historical documentary evidence

167 A large amount of detailed documentary evidence is available for China. This material
168 documents a wide range of human activities and it provides a valuable reference for the
169 present study. Information pertaining to wars was obtained from the *Tabulation of Wars in
170 Ancient China*, an appendix of the *Military History of China*, which was summarized by the
171 Editorial Committee of Chinese Military History (1985); it has been widely utilized in
172 previous research (D.D. Zhang et al., 2005, 2015). Only the ancient wars which occurred
173 within the current territory of Shanxi Province were counted in the present study. In addition,
174 fluctuations in population size are a major component of human societal evolution and
175 therefore population information was also collated and used to characterize social change.
176 Data documenting fluctuations in the population size of Shanxi Province were obtained from
177 Lu and Teng (2006).

178 4.4 Numerical analysis

179 Only taxa which were present in at least two samples with an abundance of >2 % were
180 selected for analysis. A chironomid percentage diagram was plotted using Tilia 2.0.2 (Grimm,

181 2004). Zonation of the chironomid assemblages was accomplished using stratigraphically-
182 constrained cluster analysis (CONISS) in Tilia 2.0.2 (Grimm, 2004). Both redundancy
183 analysis (RDA) and detrended correspondence analysis (DCA) were performed using R 3.2.1
184 (Team, 2014) to explore the relationship between modern chironomid taxa and temperature
185 variables, and to analyze the distribution characteristics of fossil assemblages, respectively. In
186 addition, Pearson correlation and Granger causality analysis were performed to explore the
187 relationship between climate change and the occurrence of wars.

188

189 **5 Results**

190 5.1 Modern chironomid assemblages

191 Air temperature is widely assumed to play a key role in controlling the abundance and
192 composition of chironomid taxa in freshwater (e.g., Walker, 2001; Brooks, 2003; Walker and
193 Cwynar, 2006). RDA of the chironomid taxa and temperature variables shows that TANN
194 tends to be more significant in influencing the chironomid assemblages than the mean
195 temperatures of summer, June, July and August (Fig. 3b). This result also passed the Monte
196 Carlo permutation test ($p=0.001$) even though the explanatory ability is relatively low (Fig.
197 3b). The taxa are plotted in Fig. 3c according to the taxon scores in the RDA of chironomid
198 assemblages and TANN. Taxa on the left side of the plot currently prefer a warmer
199 environment in the Gonghai Lake region because they are distributed close to the positive
200 axis of TANN in Fig. 3b; conversely, those taxa on the right side of the plot prefer a colder
201 environment.

202 The following criteria were used to identify temperature-sensitive species: (1) Those
203 located at the ends of Fig. 3c, and (2) those species previously reported as warm or cold

204 stenotherms. On the left side of the diagram, *Polypedilum nubifer*-type, *Dicrotendipes*
205 *nervosus*-type and *Tanytarsus mendax*-type have been previously reported as warm
206 stenotherms (Watson et al., 2010; Brooks and Heiri, 2013), and were defined as
207 thermophilous taxa here. *Procladius choreus*-type and *Microchironomus* were eliminated
208 because their high scores on the positive axis may be because in the Gonghai Lake region
209 they are indicators of deep water (H.P. Wang et al., 2016). On the right side of the diagram,
210 *Hydrobaenus conformis*-type, *Psectrocladius sordidellus*-type, and Chironomini 1st instar
211 (probably *Sergentia coracina*-type) have been widely regarded as cold stenotherms (Cranston
212 et al., 1983; Brodin, 1986; Brooks and Heiri, 2013), and were defined as cold-water taxa here.
213 *Chironomus gonghai*-type was included given that it was located at the end of the diagram
214 and tends to live in cold environments (see Fig. 5 in H.P. Wang et al., 2016).

215

216

217

Figure 3

218

219

220 5.2 Chironomid assemblages in Gonghai Lake

221 44 major taxa within 25 genera and 4 subfamilies (Tanypodinae, Chironomini, Tanytarsini
222 and Orthocladiinae) were identified, and 3 chironomid assemblage zones were recognized
223 (Fig. 4). 95.7% of the chironomid head capsules were identified to genus or species
224 morphotype. Due to poor preservation, the remaining 4.3% were only identified to subfamily
225 level; this was especially applicable to the head capsules of the tribe Tanypodinae because the
226 key identification segments of fragmented subfossils were often covered by other material.
227 The concentration of chironomid head capsules appeared to follow variations in the organic

228 matter content of the samples. The concentration was high before 1500 cal yr BP and then
229 decreased to very low values until the present (Fig. 4). The chironomid assemblage zones are
230 described below.

231 *Zone 1 (ca. 4000-2700 cal yr BP)*. This zone is dominated by *Cladotanytarsus mancus*-type,
232 *Procladius* and *Stictochironomus*. Many Tanytarsini taxa, including *Tanytarsus* ‘no spur’,
233 *Tanytarsus mendax*-type, *Tanytarsus lugens*-type and *Tanytarsus glabrescens*-type, are present
234 at a low abundance.

235 *Zone 2 (ca. 2700-1270 cal yr BP)*. This zone is characterized by the rapid decrease in the
236 abundance of *Cladotanytarsus mancus*-type and by the sudden appearance of *Parakiefferiella*
237 *bathophila*-type. In addition, there is an increasing representation of *Paratanytarsus*,
238 *Hydrobaenus conformis*-type and *Psectrocladius sordidellus*-type.

239 *Zone 3 (ca. 1270-present)*. This zone is characterized by a significant increase in
240 *Cladotanytarsus mancus*-type and a decrease in *Parakiefferiella bathophila*-type.
241 *Hydrobaenus conformis*-type remains at a relatively high level throughout the zone. There are
242 large fluctuations in the representation of most of the taxa and therefore the zone is divided
243 into the following subzones.

244 *Subzone 3a (ca. 1270-1040 cal yr BP)*. This subzone is characterised by an abrupt increase
245 of *Cladotanytarsus mancus*-type and decrease of *Parakiefferiella bathophila*-type.

246 *Subzone 3b (ca. 1040-970 cal yr BP)*. This subzone, which only consists of two samples, is
247 dominated by *Prosilocerus jacuticus*-type, *Chironomus gonghai*-type, *Chironomini larvula*
248 (probably *Sergentia coracina*-type) and *Procladius*.

249 *Subzone 3c (ca. 970-570 cal yr BP)*. Although they are very poorly represented in the
250 previous subzone, *Cladotanytarsus mancus*-type, *Parakiefferiella bathophila*-type and

251 *Hydrobaenus conformis*-type became dominant in this subzone.

252 *Subzone 3d (ca. 570-270 cal yr BP)*. In this subzone, *Psectrocladius sordidellus*-type
253 increases abruptly and reaches its maximum abundance, and *Hydrobaenus conformis*-type is
254 highly abundant throughout.

255 *Subzone 3e (ca. 270 cal yr BP-present)*. The dominant taxon in this subzone is
256 *Paratanytarsus penicillatus*-type. Both *Cladotanytarsus mancus*-type and *Glyptotendipes*
257 *severini*-type increase slightly, whereas *Hydrobaenus conformis*-type and *Psectrocladius*
258 *sordidellus*-type decrease significantly.

259

260

261

Figure 4

262

263

264 **5.3 Changes in the abundance of temperature indicator species**

265 Based on the definition of warm- and cold-preference taxa given above, their totals were
266 calculated to reconstruct temperature changes during the past 4000 years (Fig. 4). The results
267 indicate an overall trend of decreasing temperature; furthermore, fluctuations in the
268 abundance of cold-preference taxa indicate that the temperature was high in zone 1, decreased
269 sharply around 2700 cal yr BP but remained relatively high in zone 2, and fluctuated
270 significantly and reached a minimum in zone 3. It should be noted that the abundance of
271 warm-preference taxa is much less than that of cold-preference taxa, and the former were
272 often absent during the past 2700 years (Fig. 4). To avoid the potential limitations of

273 presence/absence data, the changes in abundance of cold-preference taxa (which provide
274 more detailed information about temperature variations on a centennial timescale) were
275 primarily used to investigate temperature changes.

276 5.4 Wars and population changes

277 We calculated a total of 418 wars from 718 BC to 1911 AD. Given that the resolution of the
278 Gonghai Lake samples ranges from 50-100 years, the incidences of wars were summed to
279 produce a 50 year-resolution. The record of chironomid-inferred temperature variability (Fig.
280 5a) and the pollen-based precipitation reconstruction for Gonghai Lake (Fig. 5b; F.H. Chen et
281 al., 2015) were compared with the cumulative frequency of these events (Fig. 5c). The
282 distribution of wars reveals that they occurred more frequently when temperature and
283 precipitation decreased abruptly, and they also lasted for a relatively long time (Fig. 5c). For
284 example, these events were the most severe during the Little Ice Age (LIA) when both the
285 temperature and precipitation decreased significantly, which lasted for nearly 350 years. The
286 results of Pearson correlation and Granger causality analysis show that the change in
287 abundance of the cold-preference taxa are significantly related to the incidence of wars
288 ($r=-0.189$ in Table 1, $p<0.01$ in Table 2).

289 Only 19 records of population size in Shanxi Province since 340 BC are mentioned in Lu
290 and Teng (2006), and they were used in the present study. These data are evenly distributed
291 within each dynasty (Fig. 5d). Although the population size fluctuated significantly, an overall
292 increasing trend is evident, together with frequent population collapses following intervals
293 with a significant number of wars.

294

295

296

Figure 5

297

298

299

300

Table 1

301

302

303

304

Table 2

305

306

307 6 Discussion

308 6.1 Effects of temperature on the modern and fossil chironomids in the Gonghai Lake

309 region

310 Relevant physical, chemical and climatic variables were all included in the investigation of
311 the relationships between chironomid assemblages and environmental parameters in the
312 Gonghai Lake region (H.P. Wang et al., 2016). Although previous analysis indicated that the
313 fossil chironomids mainly responded to changes in precipitation through water depth since the
314 last deglaciation (H.P. Wang et al., 2016), the existence of certain typical stenothermic taxa
315 provides a high potential for extracting a temperature signal. To further verify whether the
316 stenothermic taxa (based on the published literature) also have a thermal significance in the
317 Gonghai Lake region, the temperature variables (TANN, summer Tem, June Tem, July Tem
318 and August Tem) were used as the only variables to constrain the changes in the abundance of

319 the taxa in the calibration set. The results of RDA of modern chironomid assemblages and
320 temperature variables (Fig. 3b), as well as the Monte Carlo permutation test, demonstrate that
321 TANN was a significant environmental variable influencing the modern chironomid taxa. In
322 addition, TANN has a higher score on the first axes than the other variables in Fig. 3b,
323 furthermore, TANN was the only variable selected in the interactive-forward-selection
324 ($p=0.026$). This result has rarely been observed in the published literature, although it has
325 been noted that chironomids often respond significantly to mean July or summer temperature
326 (e.g., Brooks and Birks, 2001; Self et al., 2011; Samartin et al., 2017). Our observed
327 correlation between modern chironomid assemblages and TANN provides a valuable
328 reference for extracting temperature signals from the fossil chironomid assemblages of
329 Gonghai Lake. For example, *Chironomus gonghai*-type is ranked at the end of the RDA of the
330 modern assemblage data and TANN, indicating that it is cold-temperature indicator in the
331 Gonghai Lake region. Moreover, this taxon was abundant during the Younger Dryas, clearly
332 indicating that it prefers a cold environment. However, *Chironomus* is reported as a temperate
333 indicator in chironomid records from Scotland and northern Russia (e.g., Brooks et al., 2007;
334 Brooks et al., 2012b; Nazarova et al., 2015). The reason for these contradictory findings may
335 be that *Chironomus gonghai*-type is a new species, or that *Chironomus* has a different
336 preference in the Gonghai Lake region. These observations indicate that it is necessary to
337 improve the taxonomic resolution of chironomid identifications and to establish more
338 precisely the environmental preferences of chironomid taxa from local training sets to
339 enhance the reliability of paleotemperature reconstructions.

340 6.2 Faunistics and inferred temperature change

341 Temperature variability in the Gonghai Lake region during the past 4000 years is revealed
342 by changes in the abundance of the warm-preference and cold-preference chironomid taxa
343 (Fig. 4). As described in section 5.3, the variations in the abundance of the cold-preference

344 taxa were primarily used to investigate the temperature changes. An explanation for the more
345 resolved temperature signal carried by the cold-preference taxa may be that they were easily
346 able to become dominant in Gonghai Lake and respond quickly to temperature fluctuations
347 due to the lake's relatively high-elevation (1860 m a.s.l.) and the decreasing trend of late
348 Holocene temperature.

349 In addition to the warm- and cold-preference taxa, there are other chironomid taxa in the
350 Gonghai Lake record which could also be regarded as temperature indicators (although to a
351 significantly lesser extent) and it is worth investigating whether they exhibit a similar trend of
352 temperature change to the warm- and cold-preference taxa. Details of the faunistics and
353 inferred environmental change for each of the three intervals of the record are given below.

354 *4000-2700 cal yr BP.* During this interval, the temperate-preferring taxon *Cladotanytarsus*
355 *mancus*-type (Brooks, 2006) is dominant. Thus, we infer that the temperature was relatively
356 high during this interval. *Stictochironomus* and *Procladius* were abundant in this stage as well
357 as in the mid-Holocene (H.P. Wang et al., 2016), and this may indicate a relatively warm
358 environment in this stage. This is similar to a record from Norway which showed that
359 *Stictochironomus* and *Procladius* indicate a relatively warm environment (Brooks and Birks,
360 2000).

361 *2700-1270 cal yr BP.* The abundance of the previously dominant temperate-preference
362 *Cladotanytarsus mancus*-type decreased abruptly and it was replaced by *Parakiefferiella*
363 *bathophila*-type which is also a temperate-preference taxon (Brooks and Birks, 2000; Brooks,
364 2000). This shift in the representation of the dominant temperate-preference taxa probably
365 occurred in the context of cold conditions, because the cold stenotherm *Hydrobaenus*
366 *conformis*-type (Cranston et al., 1983) appears for the first time. In addition, another cold
367 indicator, *Psectrocladius sordidellus*-type (Brooks and Heiri, 2013), also started to increase,
368 marking the beginning of the 2700 cal yr BP cold event. However, the abundance of

369 *Paratanytarsus penicillatus*-type, which is not usually indicative of cool temperatures, also
370 increased since 2700 cal yr BP, simultaneously with *Psectrocladius sordidellus*-type. This
371 curious combination of chironomid changes also occurred in a sediment record from
372 Gerzensee, Switzerland (Brooks and Heiri, 2013). Overall, we infer that temperature began to
373 decrease during this second stage.

374 *1270 cal yr BP-present*. The cold-preference taxa, including *Hydrobaenus conformis*-type
375 and *Psectrocladius sordidellus*-type, and cool-preference taxa *Paratanytarsus*
376 *penicillatus*-type, are dominant in this stage, while the relatively temperate-preference taxa,
377 including *Cladotanytarsus mancus*-type, *Parakiefferiella bathophila*-type and *Procladius*,
378 exhibit low abundances. Thus, we conclude that temperatures reached a minimum. Several
379 climatic events can be recognized; for example, chironomid subzones 3a, 3c and 3e
380 correspond to the Sui-Tang Warm Period (STWP), the Medieval Warm Period (MWP) and the
381 modern warm period, respectively; in addition, subzones 3b and 3d correspond to the cold
382 periods of the 5 Dynasties & 10 Kingdoms in China and the LIA, respectively.

383 The foregoing analysis indicates that the temperature variability inferred from typical
384 chironomid temperature-indicators is in accord with that inferred from most of the other taxa
385 in the Gonghai Lake sediments, which supports our reconstruction.

386 In addition, a recent study indicated that the organic matter content of the Gonghai Lake
387 sediments was dominated by the authigenic fraction during the past 4000 years (S.Q. Chen et
388 al., under review). This suggests that most of the organic matter is of within-lake origin (Birks
389 and Birks, 2006) and thus that variations in its content probably reflect past regional
390 temperature changes. The variation of the organic content of the Gonghai Lake sediments (Fig.
391 4; [S.Q. Chen et al., 2018](#)) is consistent with the decreasing trend of chironomid-inferred
392 temperature, validating the reliability of our temperature reconstruction.

393 6.3 Intraregional temperature comparison

394 As mentioned previously, climate-model simulation results indicate that TANN in China
395 was higher in the late-Holocene than in the mid-Holocene (Jiang et al., 2012). In addition,
396 even the global TANN indicates a warming trend from the early Holocene onwards, due to the
397 retreating ice sheets and rising atmospheric greenhouse gas concentrations (Z. Liu et al.,
398 2014), in contradiction to the cooling trend inferred from various proxy records for 30-90N
399 (Marcott et al., 2013). Our qualitative reconstruction of TANN in North China suggests that
400 the warming trend estimated for the late Holocene by the simulation results is not convincing.

401 To validate our chironomid-inferred temperature record (Fig. 6a), all the Holocene
402 temperature reconstructions for China were collected. However, as mentioned in the
403 **Introduction**, many of the records are problematic in that they have a large dating uncertainty,
404 low resolution or are environmentally ambiguous; for these reasons, they were excluded.
405 Only two unambiguous and high-resolution temperature reconstructions were finally chosen
406 for further comparison due to their precise high-quality dating which was the most important
407 selection criterion used in this study. The first record is based on stalagmite layer thickness at
408 Shihua Cave, close to Gonghai Lake (Tan et al., 2003) (Fig. 6b); and the second is based on
409 historical documents pertaining to winter temperature changes in Eastern China (Ge et al.,
410 2003) (Fig. 6c). The three records exhibit a consistent pattern of temperature change on both a
411 millennial and shorter scale: cold intervals from 1350-1650 cal yr BP, 950-1150 cal yr BP and
412 300-650 cal yr BP (LIA); and warm intervals from 1150-1350 cal yr BP (STWP) and 650-950
413 cal yr BP (MWP). In addition, an integrated temperature record for the whole of China,
414 produced by combining multiple paleoclimate proxy records from ice cores, tree rings, lake
415 sediments and historical documents (Fig. 6d, Yang et al., 2002), was compared with the
416 chironomid-inferred temperature record from Gonghai Lake. Both records show the same
417 pattern of warm and cold intervals during the past 2000 years: for example, the cold intervals
418 of 1350-1650 cal yr BP and 950-1150 cal yr BP, and the LIA, STWP, MWP and modern warm

419 periods.

420 In addition to the consistency of the records described above, the trend of generally
421 decreasing temperature during the past 4000 years is also evident in several other recent
422 proxy-based reconstructions: for example, the U_{37}^K record from the sediments of Gahai and
423 Qinghai Lakes in the northeastern Tibetan Plateau (He et al., 2013; Z. Wang et al., 2015), a
424 novel microbial lipid record from Dajiuhu in central China (Huang et al., 2013), percentages
425 of thermophilous trees in Huguangyan Maar Lake in southern China (S.Y. Wang et al., 2007),
426 and an integrated temperature reconstruction for 30°-90° in the Northern Hemisphere (Fig. 6e)
427 (Marcott et al., 2013). The similarity of these proxy-based temperature reconstructions to a
428 record of total solar irradiance (Fig. 6f; Steinhilber et al., 2009) and the similar decreasing
429 trend of the various reconstructions and solar insolation (Fig. 6g; Berger and Loutre, 1991)
430 suggest that solar irradiance and insolation are important external drivers of temperature
431 variability during the late Holocene at centennial and millennial scales, respectively.

432 The foregoing demonstrates that our chironomid-based temperature reconstruction is
433 reasonable and representative and that the approach can be extended to longer time-scales.
434 The success of our approach can be attributed to the following factors: (i) Chironomids are
435 sensitive to temperature changes; (ii) the precise, high-resolution chronology increases the
436 usefulness of the temperature reconstruction; and (iii) the 60 a-resolution enables the results
437 to be compared with other high-quality temperature reconstructions and with documentary
438 evidence. Furthermore, our results, combined with a pollen-based precipitation reconstruction
439 from the same core, enable the identification of trends in both temperature and humidity (Fig.
440 5b; F.H. Chen et al., 2015). Generally, there were pronounced changes in warm and
441 humid/cool and dry climatic patterns both on millennial- and centennial- scales in the
442 Gonghai Lake region, which is consistent with a previous synthesis study (Tan et al., 2011b).
443 However, this pattern is not evident during the last 300 years (Fig. 5). Given the general

444 consistency between our temperature reconstruction and other records in this period (such as
445 the rapid warming at the end of LIA, Fig. 6), more high-quality precipitation records are
446 needed to further validate this warm and dry configuration.

447

448

449

Figure 6

450

451

452 6.4 Relationship between societal crises in Shanxi Province and climate change

453 Although past wars in China were often the consequence of social-geopolitical factors,
454 including territorial disputes (Zhao, 2006), nomadic invasions, and agricultural expansion (Di
455 Cosmo, 2002), the impact of climate change should also be considered when analyzing
456 societal evolution (Ge, 2011). Traditionally, China was an agricultural society the productivity
457 of which was very low during most of its history. When temperature or precipitation
458 decreased abruptly, or fluctuated significantly, there tended to be an increase in the incidence
459 of natural disasters such as floods and droughts (Q. Zhang et al., 2008) which seriously
460 affected agricultural production. The combination of a large population and a poor grain
461 harvest often resulted in high rice prices and famines, which generated large numbers of
462 homeless refugees and outbreaks of plague. These factors would finally trigger wars and
463 social unrest which acted to reduce the population size. To analyze the societal response in
464 Shanxi Province to climate change, the occurrence of wars (Fig. 5c) and changes in
465 population size (Fig. 5d) were summarized for comparison with the chironomid-inferred
466 temperature record (Fig. 5a) and the pollen-based precipitation reconstruction (Fig. 5b; F.H.
467 Chen et al., 2015) from Gonghai Lake.

468 Although both temperature and precipitation in the Gonghai Lake region exhibit a
469 decreasing trend during the last 4000 years, temperature changes were not always in phase
470 with precipitation changes. For example, four cold events can be recognized from the
471 chironomid-inferred temperature record (Fig. 5a), which occurred during ~2180-2710 cal yr
472 BP (Spring & Autumn and Warring States Period), 1300-1690 cal yr BP (Era of Disunity),
473 900-1050 cal yr BP (5 Dynasties and 10 Kingdoms), and 300-650 cal yr BP (Ming Dynasty).
474 The reconstructed precipitation record only exhibits two dry events during this interval, from
475 900-1050 cal yr BP and from 300-650 cal yr BP. The societal response to such events varied
476 during different periods. The incidence of war was especially high during 900-1050 cal yr BP
477 and 300-650 cal yr BP when both temperature and precipitation were lower; it was higher at
478 these times than during the periods of 2180-2710 cal yr BP and 1350-1690 cal yr BP when the
479 decrease in temperature was more severe than that of precipitation. This relationship is
480 confirmed by the results of Granger causality analysis (see Table 2 in *War and population*),
481 which show that the incidence of wars is more strongly correlated with temperature changes
482 than with precipitation. However, this may only be a statistical artifact and the causal
483 relationship between climate change and societal crises needs to be further tested in future
484 research. A sharp decrease in temperature may have been an important precondition for an
485 outbreak of war in China, but it may have insufficient in isolation, and decreases in
486 precipitation during the past 3000 years may also have been important. Moreover, the fact that
487 historical documents in China became increasingly detailed and reliable as human society
488 developed (Ge et al., 2010) may be an additional explanation for the observation that
489 increases in the frequency of wars persistently coincided with decreases in temperature and
490 precipitation. With regard to population, an increase often occurred during warm periods
491 which would have created latent economic pressures when the crop harvest was poor
492 following a cold period. **In addition, population collapse often occurred following an increase**
493 **in the frequency of wars, famines and plagues during cold periods, suggesting that population**

494 size could be indirectly influenced by climate change (D.D. Zhang et al., 2011).

495 The demise of the Ming dynasty provides an example of how climatic deterioration, as well
496 as the related socioeconomic impacts, severely undermined an empire in historical China. The
497 late Ming (306-390 cal yr BP) coincided with the Little Ice Age, when temperatures decreased
498 significantly (Fig. 5a). During this cold period, the incidence of natural disasters such as flood
499 and droughts was the highest in Shanxi history (G.Y. Chen, 1939). Rapid cooling
500 accompanied by large-scale desertification began in the 1620s and had a devastating effect on
501 agricultural production (X. Wang et al., 2010; Yin et al., 2015). Zheng *et al.* (2014) noted that
502 the total grain yield in Shanxi in the 1630s ranged from 1219.8×10^6 to 1951.3×10^6 kg, a
503 reduction of almost 50% compared to the yield of ~ 1580 (2439.1×10^6 kg). The population
504 increased from 8.42 to 9.50 million during this period (Zheng et al., 2014) and it seemed that
505 widespread famines would be unavoidable given the additional factor that governmental
506 disaster relief malfunctioned due to political corruption in the late Ming (Zheng et al., 2014;
507 Xiao et al., 2015). Furthermore, the fiscal situation of the Ming was precarious since conflicts
508 with the Jurchen people soon exhausted the treasury and the government was forced to levy
509 higher taxes on the peasants (Huang, 1974; Gu, 1984; Wei et al., 2014). The exacerbation of
510 the food crisis consequently triggered a prolonged peasant uprising which broke out in
511 northern Shaanxi, spread to Shanxi, and finally overturned the Ming Empire in 1644. The
512 historical records at a provincial level are voluminous and the socioeconomic context was
513 complex and further research is needed to explore the relationship between climate change
514 and the societal response on a regional scale in China

515

516 **7 Conclusions**

517 Together with a precise high-resolution chronology and a modern calibration set, we have

518 used chironomid assemblages from the sediments of Gonghai Lake to reconstruct temperature
519 variations during the past 4000 years in northern China. Combined with historical documents,
520 the temperature record was used to explore the relationship between climate change and
521 human societal changes at the regional scale. The principal conclusions are as follows:

522 (1) The chironomid-inferred temperature record exhibits a stepwise decreasing trend since
523 4000 cal yr BP. Temperature remained high during 4000-2700 cal yr BP; decreased abruptly
524 around 2700 cal yr BP; decreased gradually from 2700-1270 cal yr BP; and reached a
525 minimum, accompanied by frequent fluctuations, during the last 1270 years. In addition, the
526 cold event, corresponding to the Era of Disunity in China, the STWP, MWP and LIA,
527 revealed in the chironomid record from Gonghai Lake, were also recorded in numerous other
528 multi-proxy records, validating the reliability of our temperature reconstruction.

529 (2) The frequency of wars in Shanxi Province during the last 2700 years is significantly
530 correlated with the chironomid-inferred temperature record from Gonghai Lake. Reductions
531 in population size, associated with warfare and famine, are also correlated with the
532 temperature fluctuations. We suggest that the impacts of temperature and precipitation on
533 human society should be further studied in the future.

534

535 **Acknowledgements.** We thank Qiang Wang and Haichao Xie for help with fieldwork, Prof.
536 Guanghui Dong and Dr. Harry F. Lee for helpful discussions, and Dr. Jan Bloemendal for
537 improving the English language. This research was jointly supported by the National Natural
538 Science Foundation of China (grants 41471162, 41790421, 41721091), the National Key
539 R&D Program of China (grant 2017YFA0603402) and Fundamental Research Funds for the
540 Central Universities (grant lzujbky-2016-271).

541 **References:**

- 542 Armitage, P.D., Cranston, P.S., and Pinder, L.C.V. (Eds): The Chironomidae. Biology and ecology of
543 non-biting midges, Chapman and Hall, London, 1995.
- 544 Berger, A. and Loutre, M.F.: Insolation values for the climate of the last 10 million years, *Quat. Sci.*
545 *Rev.*, 10(4), 297-317, 1991.
- 546 Birks, H.H. and Birks, H.J.B.: Multi-proxy studies in palaeolimnology, *Veg. Hist. Archaeobot.*, 15,
547 235-251, 2006.
- 548 Brodin, Y.W.: The postglacial history of Lake Flarken, southern Sweden, interpreted from subfossil
549 insect remains, *Int. Rev. Hydrobiol.*, 71, 371-432, 1986.
- 550 Bronk Ramsey, C.: Deposition models for chronological records, *Quat. Sci. Rev.*, 27, 42-60, 2008.
- 551 Brooks, S.J.: Late-glacial fossil midge stratigraphies (Insecta: Diptera: Chironomidae) from the Swiss
552 Alps, *Palaeogeogr. Palaeoclimatol. Palaeoecol.*, 159(3), 261-279, 2000.
- 553 Brooks, S.J.: Chironomidae (Insecta: Diptera), In: MacKay A., Battarbee R.W., Birks H.J.B., (Eds)
554 *Global change in the Holocene* Arnold, London, 2003.
- 555 Brooks, S.J.: Fossil midges (Diptera: Chironomidae) as palaeoclimatic indicators for the Eurasian
556 region, *Quat. Sci. Rev.*, 25, 1894-1910, 2006.
- 557 Brooks, S.J. and Birks, H.J.B.: Chironomid-inferred late-glacial and early-Holocene mean July air
558 temperatures for Kråkenes Lake, western Norway, *J. Paleolimnol.*, 23(1), 77-89, 2000.
- 559 Brooks, S.J. and Birks, H.J.B.: Chironomid-inferred air temperatures from Lateglacial and Holocene
560 sites in north-west Europe: progress and problems, *Quat. Sci. Rev.*, 20(16), 1723-1741, 2001.
- 561 Brooks, S.J. and Heiri, O.: Response of chironomid assemblages to environmental change during the
562 early Late-glacial at Gerzensee, Switzerland, *Palaeogeogr. Palaeoclimatol. Palaeoecol.*, 391, 90-98,
563 2013.
- 564 Brooks, S.J., Langdon, P.G., and Heiri, O.: The identification and use of Palaeartic Chironomidae
565 larvae in palaeoecology, Quaternary Research Association, London, 2007.
- 566 Brooks, S.J., Axford, Y., Heiri, O., Langdon, P.G., and Larocque-Tobler I.: Chironomids can be reliable
567 proxies for Holocene temperatures. A comment on Velle et al. (2010), *Holocene*, 22(12), 1495-1500,
568 2012a.
- 569 Brooks, S.J., Matthews, I.P., Birks, H.H., and Birks, H.J.B.: High resolution Lateglacial and
570 early-Holocene summer air temperature records from Scotland inferred from chironomid assemblages,
571 *Quat. Sci. Rev.*, 41, 67-82, 2012b.

572 Cai, Y.J., Tan, L.C., Cheng, H., An, Z.S., Edwards, R.L., Kelly, J.M., Kong, X.G., and Wang, X.F.: The
573 variation of summer monsoon precipitation in central China since the last deglaciation, *Earth Planet Sci.*
574 *Lett.*, 29, 121-131, 2010.

575 **Chen, F.H., Chen, J.H., Holmes, J., Boomer, I., Austin, P., Gates, J.B., Wang, N.L., Brooks, S.J., and**
576 **Zhang, J.W.: Moisture changes over the last millennium in arid central Asia: a review, synthesis and**
577 **comparison with monsoon region, *Quat. Sci. Rev.*, 29, 1055-1068, 2010.**

578 Chen, F.H., Xu, Q.H., Chen, J.H., Birks, H.J.B., Liu, J.B., Zhang, S.R., Jin, L.Y., An, C.B., Telford, R.J.,
579 Cao, X.Y., Wang, Z.L., Zhang, X.J., Selvaraj, K., Lü, H.Y., Li, Y.C., Zheng, Z., Wang, H.P., Zhou, A.F.,
580 Dong, G.H., Zhang, J.W., Huang, X.Z., Bloemendal, J., and Rao, Z.G.: East Asian summer monsoon
581 precipitation variability since the last deglaciation, *Sci. Rep.*, 5, 11186, 2015.

582 Chen, G.Y.: China successive natural and manmade disasters table (in Chinese), Jinan University Book
583 Series, Guangzhou, 1939.

584 Chen, J.H., Chen, F.H., Zhang, E.L., Brooks, S.J., Zhou, A.F., and Zhang, J.W.: A 1000-year
585 chironomid-based salinity reconstruction from varved sediments of Sagan Lake, Qaidam Basin, arid
586 Northwest China, and its palaeoclimatic significance, *Chin. Sci. Bull.*, 54(20), 3749-3759, 2009.

587 Chen, J.H., Zhang, E.L., Brooks, S.J., Huang, X.Z., Wang, H.P., Liu, J.B., and Chen, F.H.:
588 Relationships between chironomids and water depth in Bosten Lake, Xinjiang, northwest China, *J.*
589 *Paleolimnol.*, 51(2), 313-323, 2014.

590 Chen, J.H., Rao, Z.G., Liu, J.B., Huang, W., Feng, S., Dong, G.H., Hu, Y., Xu, Q.H., and Chen, F.H.:
591 On the timing of the East Asian summer monsoon maximum during the Holocene—Does the
592 speleothem oxygen isotope record reflect monsoon rainfall variability?, *Sci. China Ser. D Earth Sci.*, 59,
593 2328-2338, 2016.

594 **Chen, S.Q., Liu, J.B., Xie, C.L., Chen, J.H., Wang, H.P., Wang, Z.L., Rao, Z.G., Xu, Q.H., and Chen,**
595 **F.H.: Evolution of integrated lake status since the last deglaciation: a high-resolution sedimentary**
596 **record from Lake Gonghai, Shanxi, China, *Palaeogeogr. Palaeoclimatol. Palaeoecol.*, doi:**
597 **10.1016/j.palaeo.2018.01.035, 2018.**

598 Cranston, P.S., Oliver, D.R., and Saether, O.A.: The larvae of Orthocladiinae (Diptera: Chironomidae)
599 of the Holarctic region: keys and diagnoses, *Ent. Scand. Suppl.*, 19, 149-291, 1983.

600 **Dataset of monthly values of climate data from Chinese surface station:**
601 **http://data.cma.cn/data/cdcdetail/dataCode/SURF_CLI_CHN_MUL_MON.html, last access: 10**
602 **October 2017.**

603 Di Cosmo, N.: Ancient China and its enemies: The rise of nomadic power in East Asian history,
604 Cambridge University Press, Cambridge, 2002.

605 Editorial Committee of Chinese Military History: Tabulation of Wars in Ancient China (in Chinese),
606 People's Liberation Army Press, Beijing, 1985.

607 Eggermont, H., Heiri, O., Russell, J., Vuille, M., Audenaert, L., and Verschuren, D.: Paleotemperature
608 reconstruction in tropical Africa using fossil Chironomidae (Insecta: Diptera), *J. Paleolimnol.*, 43(3),
609 413-435, 2010.

610 Gao, L., Nie, J.S., Clemens, S., Liu, W.G., Sun, J.M., Zech, R., and Huang, Y.S.: The importance of
611 solar insolation on the temperature variations for the past 110 kyr on the Chinese Loess Plateau,
612 *Palaeogeogr. Palaeoclimatol. Palaeoecol.*, 317-318 (1), 128-133, 2012.

613 Ge, Q.S.: Climate change in Chinese dynasties, Science Press, Beijing, China, 2011.

614 Ge, Q.S., Zheng, J.Y., Fang, X.Q., Man, Z.M., Zhang, X.Q., Zhang, P.Y., and Wang, W.C.: Winter
615 half-year temperature reconstruction for the middle and lower reaches of the Yellow River and Yangtze
616 River, China, during the past 2000 years, *Holocene*, 13(6), 933-940, 2003.

617 Ge, Q.S., Zheng, J.Y., Hao, Z.X., Shao, X.M., Wang, W.C., and Luterbacher, J.: Temperature variation
618 through 2000 years in China: An uncertainty analysis of reconstruction and regional difference,
619 *Geophys. Res. Lett.*, 37(3), 2010.

620 Grimm, E.C.: Tilia and Tilia. Graph v. 2.0.2, Illinois State Museum, Springfield, USA, 2004.

621 Gu, C.: History of Peasant Wars in the End of the Ming Dynasty (in Chinese), Social Sciences Press,
622 Beijing, 1984.

623 He, Y.X., Liu, W.G., Zhao, C., Wang, Z., Wang, H.Y., Liu, Y., Qin, X.Y., Hu, Q.H., An, Z.S., and Liu,
624 Z.H.: Solar influenced late Holocene temperature changes on the northern Tibetan Plateau, *Chin. Sci.*
625 *Bull.*, 58(9), 1053-1059, 2013.

626 Heiri, O., Lotter, A.F., and Lemcke, G.: Loss on ignition as a method for estimating organic and
627 carbonate content in sediments: reproducibility and comparability of results, *J. Paleolimnol.*, 25,
628 101-110, 2001.

629 Heiri, O., Brooks, S.J., Birks, H.J.B., and Lotter, A.F.: A 274-lake calibration data-set and inference
630 model for chironomid-based summer air temperature reconstruction in Europe, *Quat. Sci. Rev.*,
631 30(23-24), 3445-3456, 2011.

632 Hu, C.Y., Henderson, G.M., Huang, J.H., Xie, S.C., Sun, Y., and R. Johnson, K.: Quantification of
633 Holocene Asian monsoon rainfall from spatially separated cave records, *Earth Planet Sci. Lett.*, 266(3),
634 221-232, 2008.

635 Huang, R.: Taxation and governmental finance in sixteenth-century Ming China (Vol. 4), Cambridge
636 University Press, Cambridge, 1974.

637 Huang, X.Y., Meyers, P.A., Jia, C.L., Zheng, M., Xue, J.T., Wang, X.X., and Xie, S.C.:
638 Paleotemperature variability in central China during the last 13 ka recorded by a novel microbial lipid
639 proxy in the Dajiuhu peat deposit, *Holocene*, 23(8), 1123-1129, 2013.

640 Jia, G.D., Rao, Z.G., Zhang, J., Li, Z.Y., and Chen, F.H.: Tetraether biomarker records from a
641 loess-paleosol sequence in the western Chinese Loess Plateau, *Front. Microbiol.*, 4, 199, 2013.

642 Jiang, D.B., Lang, X.M., Tian, Z.P., and Wang, T.: Considerable Model-Data Mismatch in Temperature
643 over China during the Mid-Holocene: Results of PMIP Simulations, *J. Clim.*, 25, 4135-4153, 2012.

644 Levesque, A.J., Cwynar, L.C., and Walker, I.R.: Exceptionally steep north-south gradients in lake
645 temperatures during the last deglaciation, *Nature*, 385(423-426), 1997.

646 Liu, J.B., Chen, J.H., Zhang, X.J., Li, Y., Rao, Z.G., and Chen, F.H.: Holocene East Asian summer
647 monsoon records in northern China and their inconsistency with Chinese stalagmite $\delta^{18}\text{O}$ records, *Earth*
648 *Sci. Rev.*, 148, 194-208, 2015.

649 Liu, J.B., Chen, S.Q., Chen, J.H., Zhang, Z.P., and Chen, F.H.: Chinese cave $\delta^{18}\text{O}$ records do not
650 represent northern East Asian summer monsoon rainfall, *Proc. Natl. Acad. Sci. U.S.A.*, 201703471,
651 2017.

652 Liu, Z., Zhu, J., Rosenthal, Y., Zhang, X., Otto-Bliesner, B.L., Timmermann, A., Smith, R.S., Lohmann,
653 G., Zheng, W.P., and Timm, O.E.: The Holocene temperature conundrum, *Proc. Natl. Acad. Sci. U.S.A.*,
654 111(34), 3501-3505, 2014.

655 Lu, Y. and Teng, Z.: *Zhongguo Fenshengqu Lishi Renkou Kao* (Examination of historical Chinese
656 population in various provinces and districts), Shandong Renmin Chubanshe, Jinan Shi, 2006.

657 Marcott, S.A., Shakun, J.D., Clark, P.U., Clark, P.U., and Mix, A.C.: A reconstruction of regional and
658 global temperature for the past 11,300 years, *Science*, 339(6124), 1198-1201, 2013.

659 Massferro, J. and Larocque-Tobler, I.: Using a newly developed chironomid transfer function for
660 reconstructing mean annual air temperature at Lake Potrok Aike, Patagonia, Argentina, *Ecol. Indic.*,
661 24(1), 201-210, 2013.

662 Nazarova, L., Herzschuh, U., Wetterich, S., Kumke, T., and Pestryakova, L.: Chironomid-based
663 inference models for estimating mean July air temperature and water depth from lakes in Yakutia,
664 northeastern Russia, *J. Paleolimnol.*, 45(1), 57-71, 2011.

665 Nazarova, L., Self, A.E., Brooks, S.J., van Hardenbroek, M., Herzschuh, U., and Diekmann, B.:
666 Northern Russian chironomid-based modern summer temperature data set and inference models, *Glob.*
667 *Planet Change*, 134, 10-25, 2015.

668 Peterse, F., Martínez-García, A., Zhou, B., Beets, C.J., Prins, M.A., Zheng, H.B., and Eglinton, T.I.:

669 Molecular records of continental air temperature and monsoon precipitation variability in East Asia
670 spanning the last 130,000 years, *Quat. Sci. Rev.*, 83, 76-82, 2014.

671 Peterse, F., Prins, M.A., Beets, C.J., Troelstra, S.R., Zheng, H.B., Gu, Z.Y., Schouten, S., and Damsté,
672 J.S.S.: Decoupled warming and monsoon precipitation in East Asia over the last deglaciation, *Earth
673 Planet Sci. Lett.*, 301, 256-264, 2011.

674 Rees, A.B.H., Cwynar, L.C., and Cranston, P.S.: Midges (Chironomidae, Ceratopogonidae,
675 Chaoboridae) as a temperature proxy: a training set from Tasmania, Australia, *J. Paleolimnol.*, 40(4),
676 1159-1178, 2008.

677 Reimer, P.J., Baillie, M.G.L., Bard, E., Bayliss, A., Beck, J.W., Blackwell, P.G., Ramsey, C.B., Buck,
678 C.E., Burr, G.S., Edwards, R., Friedrich, M., Grootes, P.M., Guilderson, T.P., Hajdas, I., Heaton, T.J.,
679 Hogg, A.G., Hughen, K.A., Kaiser, K.F., Kromer, B., McCormac, F.G., Manning, S.W., Reimer, R.W.,
680 and Richards, D.A.: Intcal09 and Marine09 radiocarbon age calibration curves 0-50,000 years cal BP,
681 *Radiocarbon*, 51(4), 1111-1150, 2009.

682 Rieradevall, M. and Brooks, S.J.: An identification guide to subfossil Tanypodinae larvae (Insecta:
683 Diptera: Chironomidae) based on cephalic setation, *J. Paleolimnol.*, 23, 81-99. 2001.

684 Samartin, S., Heiri, O., Joos, F., Renssen, H., Franke, J., Brönnimann, S., and Tinner, W.: Warm
685 Mediterranean mid-Holocene summers inferred from fossil midge assemblages, *Nat. Geosci.*, 10(3),
686 207-212, 2017.

687 Self, A.E., Brooks, S.J., Birks, H.J.B., Nazarova, L., Porinchu, D., Odland, A., Yang, H., and Jones, V.J.:
688 The distribution and abundance of chironomids in high-latitude Eurasian lakes with respect to
689 temperature and continentality: development and application of new chironomid-based
690 climate-inference models in northern Russia, *Quat. Sci. Rev.*, 30(9), 1122-1141, 2011.

691 Shi, Y.F., Kong, Z.C., Wang, S.M., Tang, L.Y., Wang, F.B., Yao, T.D., Zhao, X.T., Zhang, P.Y., and Shi,
692 S.H.: Mid-Holocene climates and environments in China, *Glob. Planet Change*, 7(1-3), 219-233, 1993.

693 Steinhilber, F., Beer, J., and Fröhlich, C.: Total solar irradiance during the Holocene, *Geophys. Res.
694 Lett.*, 36(19), 308-308, 2009.

695 Stocker, T.F., Qin, D.H., Plattner, G.K., Tignor, M.M.B., Allen, S.K., Boschung, J., Nauels, A., Xia, Y.,
696 Bex, V., and Midgley, P.M.: *Climate Change 2013: The Physical Science Basis. Contribution of
697 Working Group I to the Fifth Assessment Report of the Intergovernmental Panel on Climate Change*,
698 Cambridge University Press, Cambridge, 2013.

699 Tan, M., Liu, T.S., Hou, J.Z., Qin, X.G., Zhang, H.C., and Li, T.Y.: Cyclic rapid warming on
700 centennial-scale revealed by a 2650-year stalagmite record of warm season temperature, *Geophys. Res.
701 Lett.*, 30(12), 2003.

- 702 Tan, L.C, Cai, Y.J., An, Z.S., Edwards, R.L., Cheng, H., Shen, C.C., and Zhang, H.W.: Centennial-to
703 decadal-scale monsoon precipitation variability in the semi-humid region, northern China during the
704 last 1860 years: Records from stalagmites in Huangye Cave, Holocene, 21(2), 287-296, 2011a.
- 705 Tan, L.C., Cai, Y.J., An, Z.S., Yi, L., Zhang, H.W., and Qin, S.J.: Climate patterns in north central
706 China during the last 1800 yr and their possible driving force, *Climate of the Past*, 7(3), 685, 2011b.
- 707 Team, R.C.: R: A language and environment for statistical computing. Vienna, Austria: R Foundation
708 for Statistical Computing; 2014, 2014.
- 709 Walker, I.R.: Midges: Chironomidae and related Diptera. In: Smol, J.P., Birks, H.J.B., Last, W.M. (Eds),
710 Tracking Environmental Change Using Lake Sediments, Kluwer Academic Publishers, Dordrecht,
711 43-66, 2001.
- 712 Walker, I.R.: The WWW Field Guide to Fossil Midges (<http://www.paleolab.ca/wwwguide/>), 2007.
- 713 Walker, I.R. and Cwynar, L.C.: Midges and palaeotemperature reconstruction—the North American
714 experience, *Quat. Sci. Rev.*, 1911-1925, 2006.
- 715 Walker, I.R., Mott, R.J., and Smol, J.P.: Allerød-Younger Dryas Lake Temperatures from Midge Fossils
716 in Atlantic Canada, *Science*, 253(5023), 1010, 1991.
- 717 Wang, H.P., Brooks, S.J., Chen, J.H., Hu, Y., Wang, Z.L., Liu, J.B., Xu, Q.H., and Chen, F.H.:
718 Response of chironomid assemblages to East Asian summer monsoon precipitation variability in
719 northern China since the last deglaciation, *J. Quat. Sci.*, 31(8), 967-982, 2016.
- 720 Wang, S., Gong, D., and Zhu, J.: Twentieth-century climatic warming in China in the context of the
721 Holocene, *Holocene*, 11(3), 313-321, 2001.
- 722 Wang, S.Y., Lü, H.Y., Liu, J.Q., and Jörg, F.W.N.: The early Holocene optimum inferred from a
723 high-resolution pollen record of Huguangyan Maar Lake in southern China, *Chin. Sci. Bull.*, 52(20),
724 2829-2836, 2007.
- 725 Wang, X., Chen, F., Zhang, J., Yang, Y., Li, J., Hasi, E., Zhang, C., and Xia, D.: Climate, desertification,
726 and the rise and collapse of China's historical dynasties, *Hum. Ecol.*, 38(1), 157-172, 2010.
- 727 Wang, X., Wang, Z.L., Chen, J.H., Liu, J.B., Wang, H.P., Xu, Q.H., Zhang, S.R., and Chen, F.H.: On
728 the origin of the upland lake group in Ningwu Tianchi region, Shanxi Province (in Chinese with
729 English abstract), *Journal of Lanzhou University (Natural Sciences)*, 50, 208-212, 2014.
- 730 Wang, Z., Liu, Z., Zhang, F., Fu, M.Y., and An, Z.S.: A new approach for reconstructing Holocene
731 temperatures from a multi-species long chain alkenone record from Lake Qinghai on the northeastern
732 Tibetan Plateau, *Org. Geochem.*, 88, 50-58, 2015.
- 733 Watson, J.E., Brooks, S.J., Whitehouse, N.J., Reimer, P.J., Birks, H.J.B., and Turney, C.:

- 734 Chironomid-inferred late-glacial summer air temperatures from Lough Nadourcan, Co. Donegal,
735 Ireland, *J. Quat. Sci.*, 25(8), 1200-1210, 2010.
- 736 Wei, Z., Fang, X., and Su, Y.: Climate change and fiscal balance in China over the past two millennia,
737 *Holocene*, 24(12), 1771-1784, 2014.
- 738 Wen, R.L., Xiao, J.L., Chang, Z.G., Zhai, D.Y., Xu, Q.H., Li, Y.C., and Itoh, S.: Holocene precipitation
739 and temperature variations in the East Asian monsoonal margin from pollen data from Hulun Lake in
740 northeastern Inner Mongolia, China, *Boreas*, 39(2), 262-272, 2010.
- 741 Wiederholm, T.E.: Chironomidae of the Holarctic region. Keys and diagnoses. Part 1. Larvae, *Ent.*
742 *Scand. Suppl.*, 19, 1-457, 1983.
- 743 Xiao, L., Fang, X., Zheng, J., and Zhao, W.: Famine, migration and war: Comparison of climate change
744 impacts and social responses in North China between the late Ming and late Qing dynasties, *Holocene*,
745 25(6), 900-910, 2015.
- 746 Xu, Q.H., Xiao, J.L., Li, Y.C., Tian, F., and Nakagawa, T.: Pollen-based quantitative reconstruction of
747 Holocene climate changes in the Daihai Lake area, Inner Mongolia, China, *J. Clim.*, 23(11), 2856-2868,
748 2010.
- 749 Yang, B., Braeuning, A., Johnson, K.R., and Shi, Y.F.: General characteristics of temperature variation
750 in China during the last two millennia, *Geophys. Res. Lett.*, 29(9), 2002.
- 751 Yin, J., Su, Y., and Fang, X.Q.: Relationships between temperature change and grain harvest
752 fluctuations in China from 210 BC to 1910 AD, *Quat. Int.*, 355, 153-163, 2015.
- 753 Zhang, D.D., Jim, C.Y., Lin, C.S., He, Y.Q., and Lee, H.F.: Climate change, social unrest and dynastic
754 transition in ancient China, *Chin. Sci. Bull.*, 50(2), 137-144, 2005.
- 755 Zhang, D.D., Lee, H.F., Wang, C., Li, B.S., Pei, Q., Zhang, J., and An, Y.L.: The causality analysis of
756 climate change and large-scale human crisis, *Proc. Natl. Acad. Sci. U.S.A.*, 108(42), 17296-17301,
757 2011.
- 758 Zhang, D.D., Pei, Q., Lee, H.F., Zhang, J., Chang, C.Q., Li, B., Li, J., and Zhang, X.: The pulse of
759 imperial China: A quantitative analysis of long-term geopolitical and climatic cycles, *Glob. Ecol.*
760 *Biogeogr.*, 24(1), 87-96, 2015.
- 761 Zhang, E.L., Bedford, A., Jones, R., Shen, J., Wang, S.M., and Tang, H.Q.: A subfossil chironomid-total
762 phosphorus inference model for lakes in the middle and lower reaches of the Yangtze River, *Chin. Sci.*
763 *Bull.*, 51(17), 2125-2132, 2006.
- 764 Zhang, E.L., Jones, R., Bedford, A., Langdon, P., and Tang, H.: A chironomid-based salinity inference
765 model from lakes on the Tibetan Plateau, *J. Paleolimnol.*, 38(4), 477-491, 2007.

- 766 Zhang, E.L., Chang, J., Cao, Y.M., Tang, H.Q., Langdon, P., Shulmeister, J., Wang, R., Yang, X.D., and
767 Shen, J.: A chironomid-based mean July temperature inference model from the south-east margin of the
768 Tibetan Plateau, China, *Clim. Past*, 13, 185-199, 2017a.
- 769 Zhang, E.L., Chang, J., Cao, Y.M., Su, W.W., Shulmeister, J., Tang, H.Q., Langdon, P., Yang, X.D., and
770 Shen, J.: Holocene high-resolution quantitative summer temperature reconstruction based on subfossil
771 chironomids from the southeast margin of the Qinghai-Tibetan Plateau, *Quat. Sci. Rev.*, 165, 1-12,
772 2017b.
- 773 Zhang, Q., Gemmer, M., and Chen, J.: Climate changes and flood/drought risk in the Yangtze Delta,
774 China, during the past millennium, *Quat. Int.*, 176, 62-69, 2008.
- 775 Zhao, D.X.: *Warfare in Eastern Zhou and the Rise of Confucian-Legalist State (in Chinese)*, East China
776 Normal University Press, Shanghai, 2006.
- 777 Zhao, Y, Chen, F.H., Zhou, A.F., Yu, Z.C., and Zhang, K.: Vegetation history, climate change and
778 human activities over the last 6200 years on the Liupan Mountains in the southwestern Loess Plateau in
779 central China, *Palaeogeogr. Palaeoclimatol. Palaeoecol.*, 293(1), 197-205, 2010.
- 780 Zheng, J.Y., Xiao, L.B., Fang, X.Q., Hao, Z.X., Ge, Q.S., and Li, B.B.: How climate change impacted
781 the collapse of the Ming dynasty, *Clim. Change*, 127(2), 169-182, 2014.

782 **Table captions**

783 **Table 1** Results of Pearson correlation analysis of cold-preference chironomid taxa percentages,
784 reconstructed precipitation and incidence of war.

785 **Table 2** Granger causality analysis of cold-preference chironomid taxa percentages, reconstructed
786 precipitation, and incidence of war.

787 **Table 1**

		War
Cold Taxa	Pearson correlation (r)	0.571**
	Significance (p)	0.000
Precipitation	Pearson correlation (r)	-0.214
	Significance (p)	0.125

788 **. p<0.01 (2-tailed)

789

790 **Table 2**

Null Hypothesis	F	p
COLD TAXA do not Granger Cause WAR	16.4887	0.0002**
PRECIPITATION does not Granger Cause WAR	0.96106	0.3317

791 **. p<0.01

792 **Figure captions**

793 **Figure 1** (a) Location of Gonghai Lake (blue dot) and other temperature records in North China. (b)
794 Location of sediment core GH09B. **Mountain (Mid and High)** indicates the area above 1000 m.a.s.l.
795 **The position of the modern Asian summer monsoon boundary is after F.H. Chen et al. (2010).**

796 **Figure 2** Age-depth model for core GH09B (F.H. Chen et al., 2015).

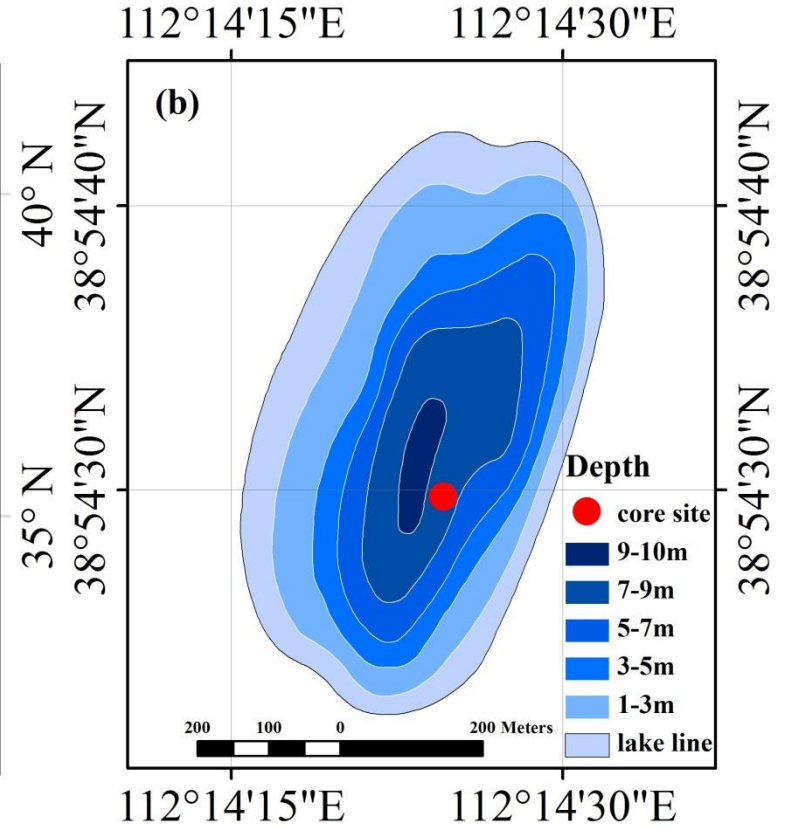
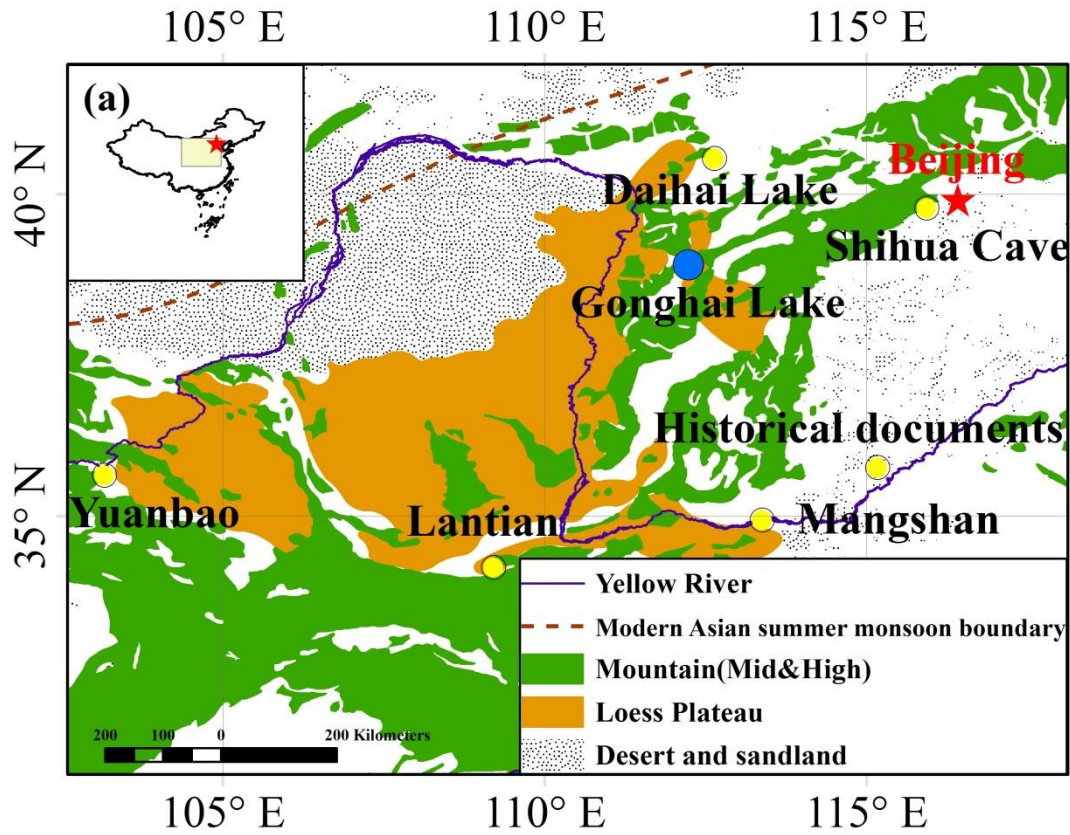
797 **Figure 3** Information about the modern calibration data set obtained from the Gonghai Lake area. (a)
798 Location of modern surface samples (white dots); (b) RDA bi-plot of modern chironomid assemblages
799 and TANN, summer Tem, June Tem, July Tem and August Tem; and (c) relative abundance of modern
800 chironomid assemblages from the modern calibration set (H.P. Wang et al., 2016). All taxa are arranged
801 according to their RDA 1 scores of chironomids and TANN. Only taxa occurring in at least two
802 samples with an abundance of >2 % are plotted.

803 **Figure 4** Relative abundance of the main chironomid taxa from Gonghai Lake during the past 4000
804 years. Taxa are plotted from left to right in order of their DCA 1 scores. Loss-on-ignition (LOI) values,
805 chironomid concentration, percentages of warm- and cold-preference taxa are plotted as red lines with
806 squares, black bars, and red and blue patterns, respectively. Three chironomid assemblage zones were
807 defined by CONISS results.

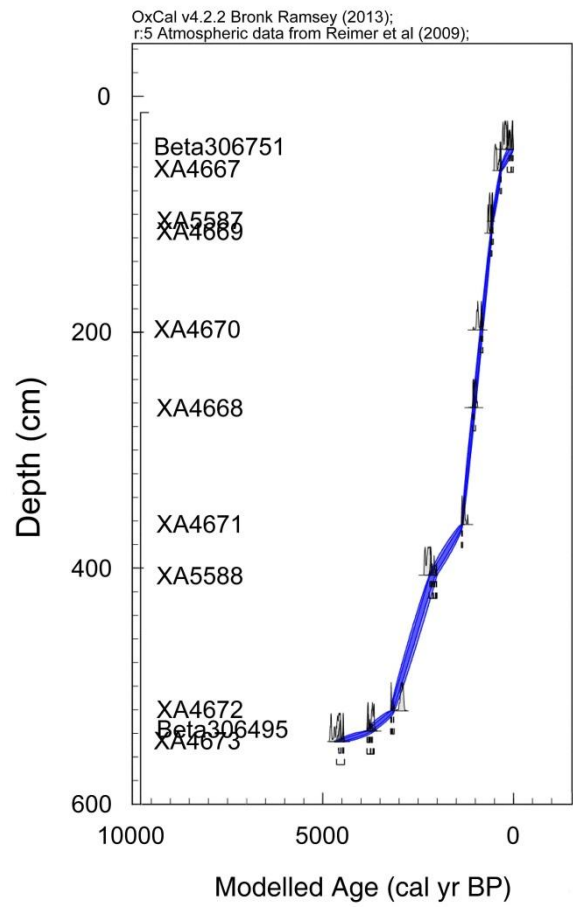
808 **Figure 5** Comparison of (a) cold-preference taxa percentages and (b) reconstructed precipitation at
809 Gonghai Lake (F.H. Chen et al., 2015) with (c) frequencies of wars in Shanxi Province, China and (d)
810 population size (in units of 1 million, square dots) of Shanxi Province during the past 2300 years; the
811 data are spline connected. **Grey shaded areas indicate cold events.**

812 **Figure 6** Comparison of (a) cold-preference taxa percentages in Gonghai Lake with intraregional
813 temperature records during the past 4000 years, including (b) reconstructed temperature based on
814 stalagmite layer thickness in Shihua Cave (Tan et al., 2003), (c) winter half-year temperature anomalies
815 in eastern China with a 30-year resolution (Ge et al., 2003), (d) weighted temperature reconstruction
816 for China obtained by combining multiple paleoclimate proxy records (Yang et al., 2002), (e) and the

817 paleotemperature for 30°-90° of the Northern Hemisphere (Marcott et al., 2013). The higher values
818 from (a) to (e) represent warmer environments, and vice-versa. All the temperature records are
819 compared with (f) a reconstruction of total solar irradiance (Steinhilber et al., 2009) and summer
820 insolation at 65°N (Berger and Loutre, 1991) during the past 4000 years. Grey shaded areas indicate
821 cold events.
822

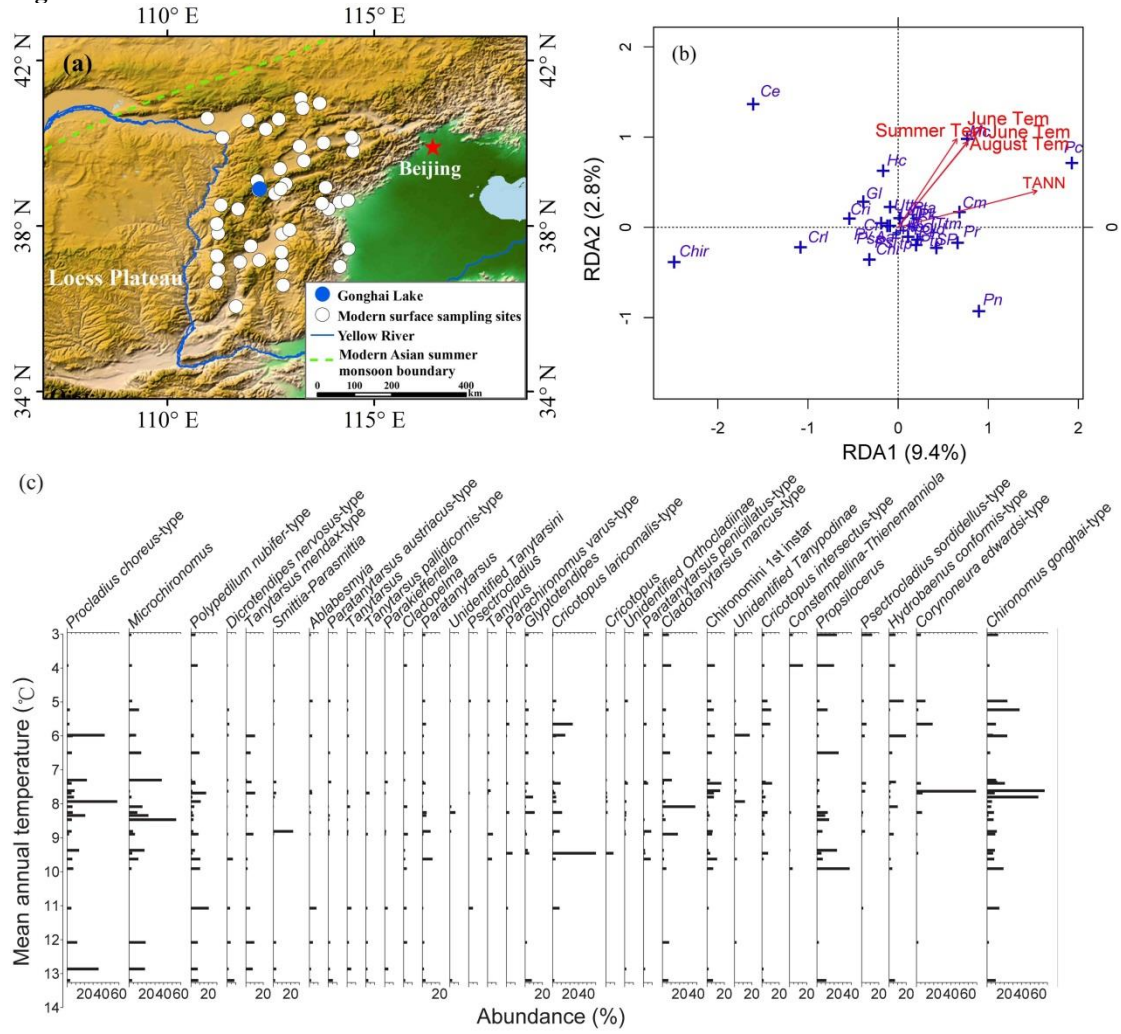


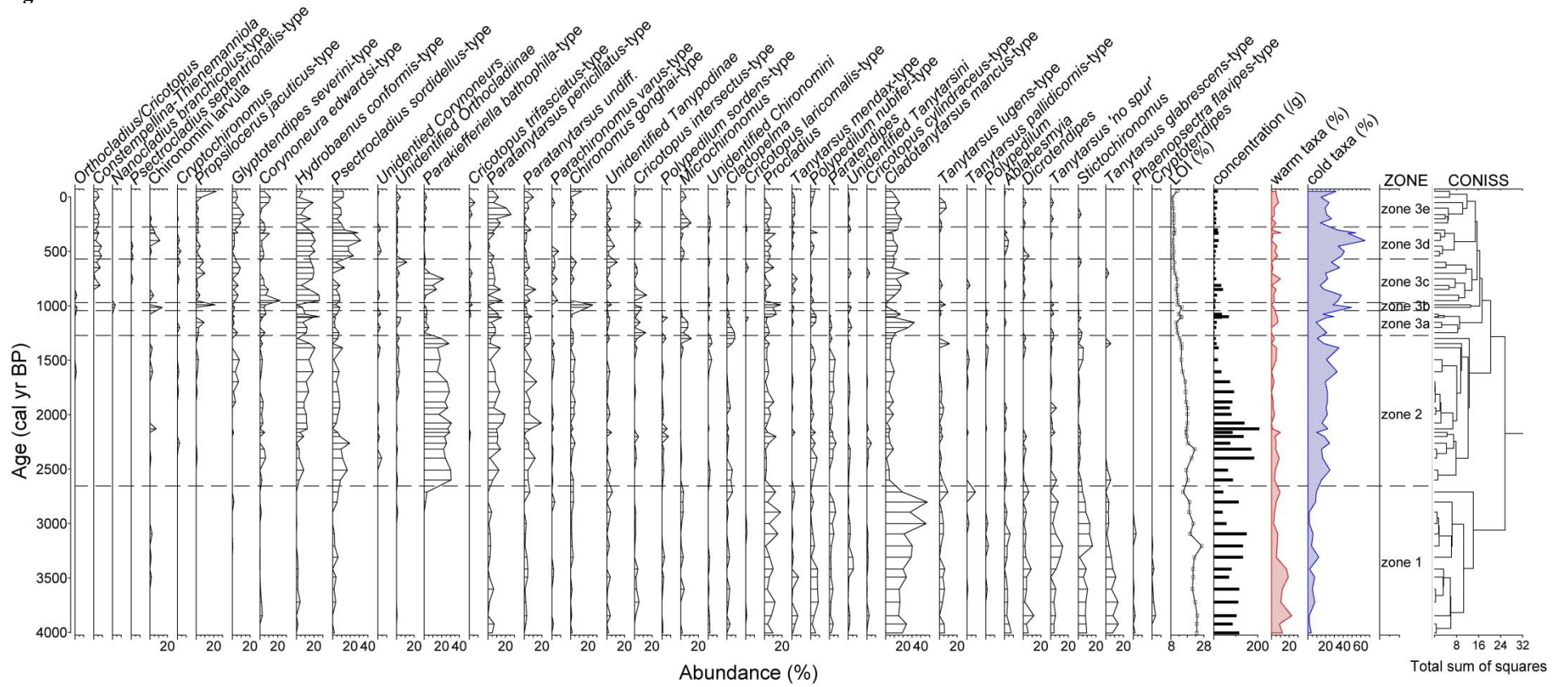
825 Fig. 2



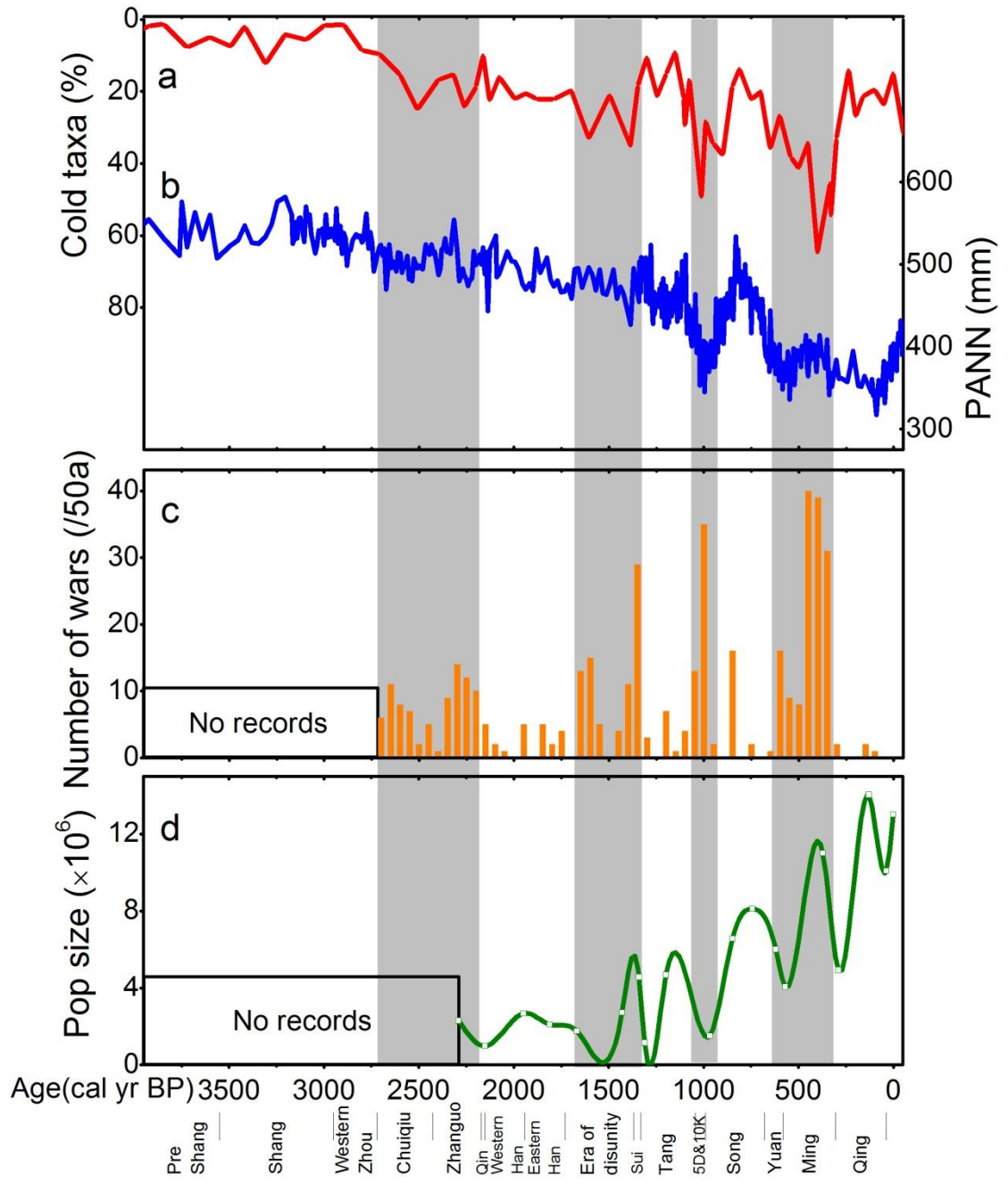
826

Fig. 3





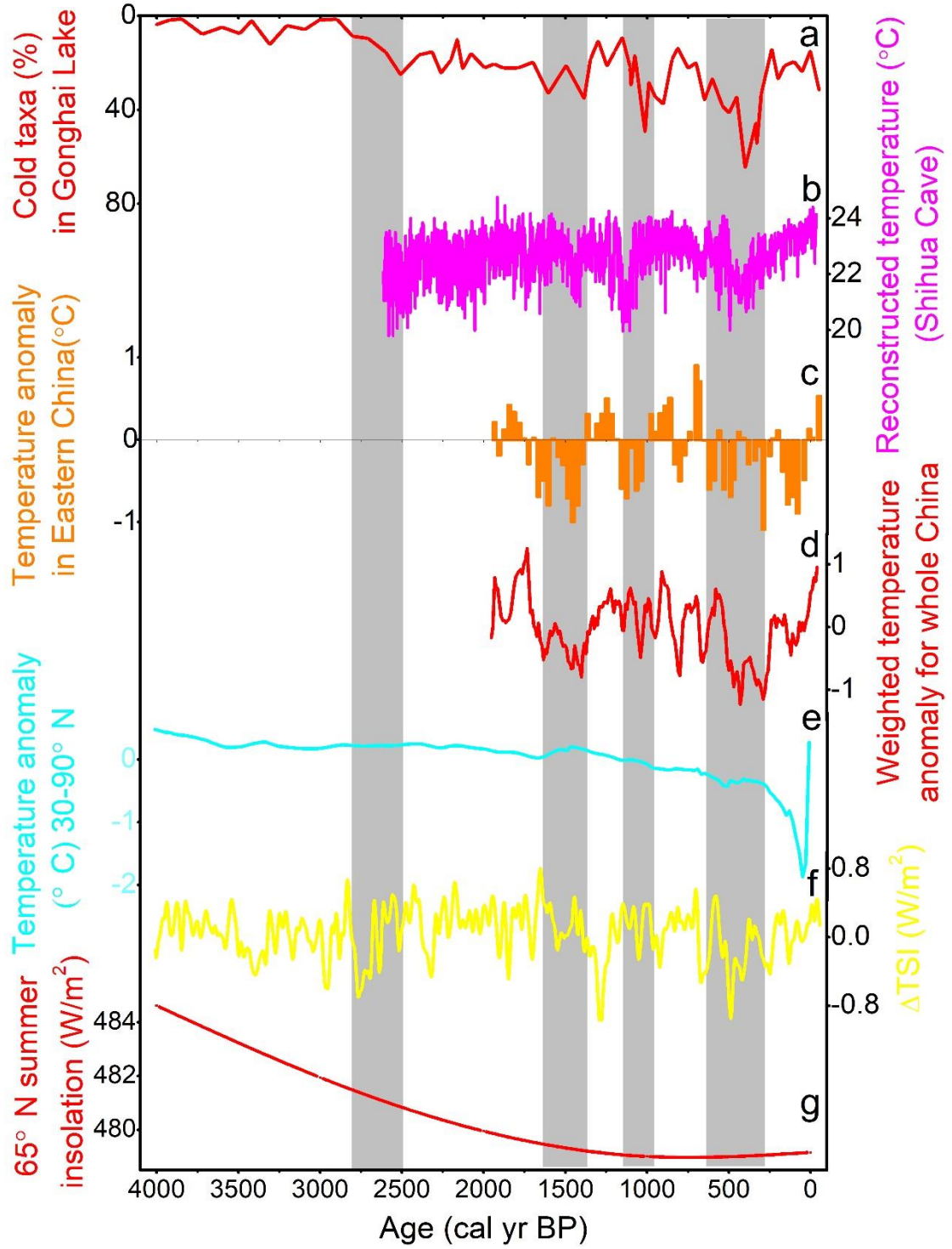
831 Fig. 5



832
833

834

Fig. 6



835